Author/s:
Vaid, TM;Chalmers, DK;Scott, DJ;Gooley, PR

Title:
INPHARMA-Based Determination of Ligand Binding Modes at α1-Adrenergic Receptors Explains the Molecular Basis of Subtype Selectivity

Date:
2020-09-10

Citation:
Vaid, T. M., Chalmers, D. K., Scott, D. J. & Gooley, P. R. (2020). INPHARMA-Based Determination of Ligand Binding Modes at α1-Adrenergic Receptors Explains the Molecular Basis of Subtype Selectivity. Chemistry A European Journal, 26 (51), pp.11796-11805. https://doi.org/10.1002/chem.202000642.

Persistent Link:
https://hdl.handle.net/11343/276164

Title: INPHARMA based determination of ligand binding modes at α1-adrenergic receptors explains the molecular basis of subtype selectivity

Authors: Tasneem M. Vaid; David K. Chalmers; Daniel J. Scott; Paul R. Gooley

To be cited as: 10.1002/chem.202000642

Link to VoR: https://doi.org/10.1002/chem.202000642

INPHARMA based determination of ligand binding modes at α_1-adrenergic receptors explains the molecular basis of subtype selectivity

Tasneem M. Vaid,[a,b,c] David K. Chalmers,[d] Daniel J. Scott*[a,c] and Paul R. Gooley*[a,b]

[a] Dr. T. M. Vaid, Prof. P. R. Gooley, Dr. D. J. Scott
Department of Biochemistry and Molecular Biology
University of Melbourne
Parkville, 3010 VIC, Australia
E-mail: prg@unimelb.edu.au, daniel.scott@florey.edu.au

[b] Dr. T. M. Vaid, Prof. P. R. Gooley
Bio21 Molecular Science & Biotechnology Institute
University of Melbourne
Parkville, 3010 VIC, Australia

[c] Dr. T. M. Vaid, Dr. D. J. Scott
The Florey Institute of Neuroscience & Mental Health
University of Melbourne
Parkville, 3015 VIC, Australia

[d] Dr. D. K. Chalmers
Monash Institute of Pharmaceutical Sciences
Monash University
Parkville, 3052 VIC, Australia

Supporting information for this article is given via a link at the end of the document.

Abstract: The structural poses of ligands that bind weakly to protein receptors are challenging to define. In this work we have studied ligand interactions with the adrenoreceptor (AR) subtypes, α_{1A}-AR and α_{1B}-AR which belong to the G-protein coupled receptor (GPCR) superfamily by employing the solution-based ligand-observed NMR method INPHARMA (Interligand Noes for PHARmacophore Mapping). Lack of receptor crystal structures and of subtype-selective drugs has hindered the definition of the physiological roles of each subtype and limited drug development. We determined the binding pose of the weak binding α_{1A}-AR selective agonist, A-61603, relative to an endogenous agonist, epinephrine, at both α_{1A}-AR and α_{1B}-AR. The NMR experimental data were quantitatively compared, using SpINPHARMA, to the back-calculated spectra based on ligand poses obtained from all-atom molecular dynamics simulations. The results helped mechanistically explain the selectivity of (*R*)-A-61603 towards α_{1A}-AR, demonstrating an approach for targeting subtype selectivity in ARs.

Introduction

G-protein coupled receptors (GPCRs) represent the largest family of human membrane proteins with more than 800 members. All GPCRs share a typical architecture of seven transmembrane (TM) spanning helices, connected by three extracellular and three intracellular loops. Extracellularly, GPCRs can detect a diverse array of molecules, ranging from small hormones and neurotransmitters to proteins such as chemokines. Extracellular ligand binding triggers structural changes throughout the receptor, which initiates a variety of intracellular signalling cascades, mediated by the binding of G proteins, arrestins and other signalling proteins.[1] These effects can be modulated, induced or blocked by drugs. In fact, GPCRs represent the largest family of proteins to which drugs are targeted.[2]

The Adrenergic receptor, or adrenoceptor (AR), GPCR family consists of nine receptor subtypes (α_{1A}-AR, α_{1B}-AR, α_{1D}-AR, α_{2A}-AR, α_{2B}-AR, α_{2C}-AR, β_1-AR, β_2-AR, β_3-AR), all of which bind the same endogenous ligands, epinephrine and norepinephrine. The α_1-AR subfamily primarily mediate norepinephrine-induced smooth muscle contraction[3] and are clinically targeted by alpha blockers (i.e. alpha-adrenergic antagonists) for the treatment of several conditions such as hypertension, Raynaud's disease (a condition resulting in a reduced blood flow caused by arterial spasms) and benign prostatic hyperplasia (BPH, an enlargement of the prostate gland).[4] In humans, α_{1A}-ARs are known to be preferentially expressed in the cerebellum, cerebral cortex, heart and prostate; α_{1B}-ARs in the aorta and spleen and α_{1D}-ARs in aorta.[5] The lack of subtype-selective ligands, however, has hindered research of subtype-specific localization and understanding of the physiological roles of each subtype. Studies on transgenic mouse models demonstrate that α_{1A}-AR and α_{1B}-ARs mediate opposing responses to epinephrine and norepinephrine release in relation to cardioprotection, seizures and neurogenesis.[3] Such opposing responses suggest that subtype selective activation (of α_{1A}-AR) or blocking (of α_{1B}-AR) may have clinical utility for treating heart failure, epilepsy and neurodegenerative diseases.[3] Molecular targeting of α_{1A}-AR and α_{1B}-AR has been hindered substantially due to their highly similar sequences (amino acid similarity in the TM region is ~87% and in the orthosteric binding region is ~90%) and a lack of structural knowledge on how ligands bind α_1-ARs. Only the structures of β-ARs have been solved to date, and the majority

of these are complexed with high affinity ligands.[6] Such ligands stabilize the receptors in specific conformational states to facilitate crystallization. Most AR agonists are, however, weakly binding ligands. To study or detect such transiently formed weak interactions, high concentrations of receptors need to be produced, which is not easily achievable with GPCRs, making detailed structural studies by the common techniques, such as X-ray crystallography, challenging. NMR spectroscopy on the other hand, is a structural technique that can obtain atomic details of weakly interacting ligands often with relatively dilute concentrations of receptor.[7]

NMR methods used to study protein-ligand interactions can be broadly classified into two groups: protein-observed and ligand-observed. In protein-observed NMR methods, the binding of the ligand is observed by intensity and chemical shift perturbations of protein resonances and information on the binding epitope of the protein and the dissociation constant (K_D) can be inferred. In ligand-observed NMR, ligand binding to the receptor is monitored by observing the NMR signals of the ligand. These experiments are performed with excess of ligand over protein (> 10:1) and the interactions observed are in the fast-exchange regime (i.e. moderate to weak affinity ligands with $k_{off} > 10^2$ s^{-1}). Under these conditions, the NMR signal of the ligand in its free state, reflects a trace memory recorded on the ligand magnetization when it was bound to the target protein. Typical experiments performed include Saturation Transfer Difference (STD) NMR,[8] water-Ligand Observed via Gradient SpectroscopY (waterLOGSY)[9] and Transferred Nuclear Overhauser Effect SpectroscopY (Tr-NOESY).[10] STD-NMR and waterLOGSY are based on the transfer of NOEs to the protons of weakly binding ligand. In the case of STD, receptor protons are selectively saturated by weak radio frequency (RF) irradiation. The magnetization is then transferred to the bound ligands via NOE.[8] In the case of WaterLOGSY, protons of bulk water are excited, and magnetization is transferred from transiently bound water molecules to the ligands.[9] These experiments have been used for the study of GPCR-ligand interactions; STD-NMR has been used for fragment screening on A_{2A} adenosine receptor ($A_{2A}R$)[11] and for the determination of the bound conformations and epitope mapping of ligands on Human Sweet Receptor,[12] C-X-C chemokine receptor type 4 (CXCR4)[13] and α_{1A} and α_{1B}-AR;[14] both STD-NMR and waterLOGSY have been used to determine the receptor-bound conformation of a peptide to CXCR4 directly on a living cell.[15]

The Tr-NOESY method is used to define the conformation of the bound ligand by observing intraligand NOE peaks between protons of the free ligand.[10, 16] These experiments use the sign inversion of the intraligand NOE cross-peaks to screen for the potential binding of small ligands. Providing the ligand experiences sufficiently long residence times, the observed negative NOEs in the Tr-NOESY are consistent with the macromolecular condition and provide structural (intraligand ^{1}H NOEs) information describing the conformation of the bound ligand.[10] Tr-NOESY, along with STD-NMR, have been used for the determination of structural features involved in the activation of $G\alpha_s$ by the PTH receptor (PTH1R).[17] If this experiment is conducted on two ligands binding to the same receptor molecule, and the ligands bind simultaneously with similar residence times, in adjacent sites on the protein surface as a ternary complex, negative interligand NOEs can be observed, which are referred to as ILOEs (Intermolecular Ligand-ligand nOE).[18] In another scenario for the binding of two ligands to the same receptor molecule, if the ligands bind competitively (and not simultaneously) with similar residence times to the same protein binding pocket, interligand NOEs can also be observed between ligand protons. Such NOESY cross-peaks are referred to as INPHARMA (Interligand Noe for PHARMAcophore) NOEs.[19] Importantly, ILOEs are generated by direct dipolar interactions between ligand protons, whereas INPHARMA NOEs are generated via magnetization passing from ligand protons to protein protons and subsequently to protons of the second ligand. Using these methods, if the binding mode of one of the compounds is known, the protein-bound orientation and structure of the other can be inferred. For GPCRs, such INPHARMA experiments were first reported on GPR40 containing cell membrane preparations[20] and more recently on human $A_{2A}R$ reconstituted in nanodiscs.[21]

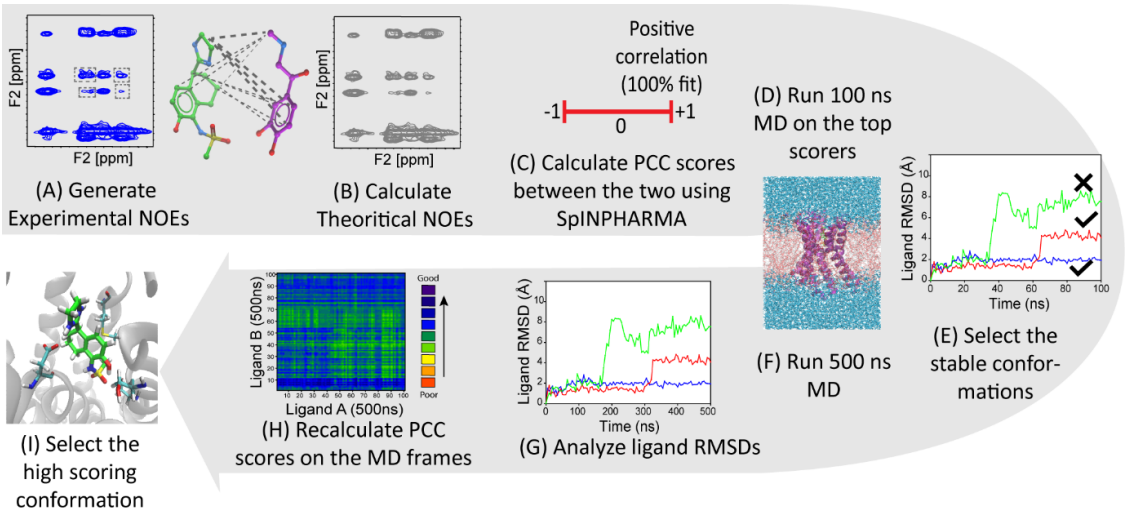

Figure 1. Flow chart illustrating the NMR-computational procedure. (A) 2D tr-NOESY spectra with the two ligands (adrenaline and A-61603) are acquired in the presence of the receptor. (B) The two ligands are docked to the homology models of the receptors. For adrenaline one docked conformation was created and for A-61603, both enantiomers (*R*)- and (*S*)-A-61603 were docked generating 30 conformations of each. (C) INPHARMA Pearson correlation coefficient (PCC) scores are calculated for all poses; high scoring poses and the lowest scoring pose (as a control) are selected. (D) 100 ns MD simulations are run. (E) For stable

simulations or those that are stabilizing, ligand RMSD values evaluated and poses are selected. (F) 500 ns simulation are run. (G) Ligand RMSDs are evaluated. (H) 100 frames from the final 250 ns of the 500 ns trajectories are extracted and INPHARMA PCC scores calculated for all 100 conformations against 100 conformations of epinephrine are displayed in heatmap plots. (I) Conformations showing the highest overall PCC scores are selected as the final bound conformation of (*R*)- and (*S*)-A-61603.

The binding of catecholamines, epinephrine and norepinephrine, to α_1-ARs has been widely explored using a number of biophysical and structure-function studies[14, 22] but there are no crystal structures available. We can infer ligand orientation and binding site from the pioneering work on the epinephrine bound structures of β_2-AR.[23] A-61603 is an α_{1A}-AR selective agonist[24] and unlike epinephrine, the structure-activity relationships (SARs) for binding of A-61603 to α_1-ARs has not been explored. Towards understanding A-61603 binding our group used STD-NMR experiments to map the binding epitope of A-61603 on α_{1A} and α_{1B}-ARs.[14] Here, we have used INPHARMA to characterize the binding of A-61603 relative to epinephrine/norepinephrine using thermostabilized variants of the α_{1A}- and α_{1B} ARs.[25] While these mutant receptors are inactive, they are binding competent and serve as excellent targets for ligand screening experiments. The INPHARMA experiments are complemented with molecular docking and atomic-level molecular dynamics (MD) simulations. The NMR-computational workflow is illustrated in the flow chart shown in Figure 1. These studies have enabled us to identify subtle structural variations within the ligand binding pockets across the closely related subtypes, information that can be used to guide structure-based and ligand-based drug design (SBDD and LBDD).

Table 1. Chemical structures of the ligands: epinephrine, norepinephrine and A-61603.

Ligand	Structure [a]
(*R*) - Epinephrine	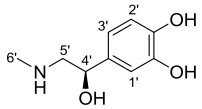
(*R*) - Norepinephrine	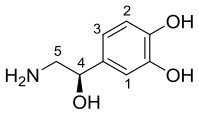
(*R/S*) - A-61603	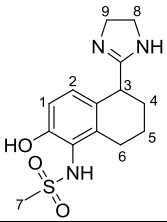

[a] Numbering indicates positions of the assigned protons in the NMR spectra (Figure S1)[14]. C3 in A-61603 is a chiral center.

Results

Tr-NOESY of ligands binding to α_{1A}-AR and α_{1B}-AR. The test ligands selected for the study are displayed in Table 1. Epinephrine and norepinephrine are endogenous ligands for α_1-ARs, whereas A-61603 is an α_{1A}-AR selective agonist. Tr-NOESY spectra were recorded for each ligand separately, in the absence or presence of either α_{1A}-AR A4 or α_{1B}-AR #15 (Figure 2). In the absence of receptor, all ligands exhibited cross-peaks characteristic of positive NOEs indicating the fast tumbling expected for small molecules. Upon addition of the receptor (either α_{1A}-AR A4 or α_{1B}-AR #15) negative ligand NOEs were observed, characteristic of the receptor-bound, macromolecular condition. NOEs between the ligand protons and water were also observed, suggesting the presence of water molecules in the binding pocket of the receptor. The variations in the intensities of the NOEs upon binding to the receptors likely indicate conformational preferences of the bound ligand at the two receptor subtypes.

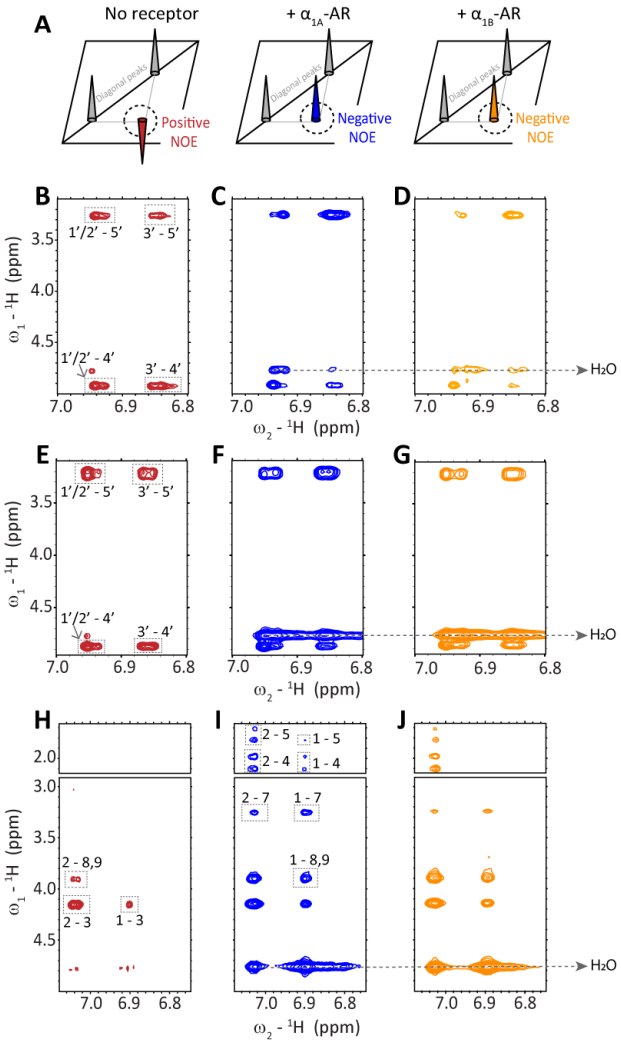

Figure 2. 2D Tr-NOESY experiments showing conformational preferences of ligands binding to the receptor. (A) The colour of the cross peak indicates the phase, positive NOEs (cross-peaks that are of opposite sign to the diagonal peaks) dark-red; negative NOEs (cross-peaks with the same sign as the diagonal peaks) blue (α_{1A}-AR A4) and orange (α_{1B}-AR #15). Epinephrine in the absence of receptor (B), in the presence of α_{1A}-AR A4 (C) and in the presence of α_{1B}-AR #15 (D). Norepinephrine in the absence of receptor (E) in the presence of α_{1A}-AR A4 (F) and in the presence of α_{1B}-AR #15 (G). A-61603 in the absence of receptor (H), in the presence of α_{1A}-AR A4

(I) and in the presence of α_{1B}-AR #15 (J). All resonances are labeled according to the structures in Table. 1. Spectra in the absence of the receptor were recorded with mixing times 800 ms while in the presence of the receptor, the spectra were acquired at 150 ms (for epinephrine) and 300 ms (for norepinephrine and A61603).

Catecholamine and A-61603 INPHARMA at α_{1A}-AR and α_{1B}-AR. The STD-NMR recorded in the presence of epinephrine or norepinephrine with A-61603, in the presence of either α_{1A}-AR A4 or α_{1B}-AR #15 show well resolved STD signals for both ligands (Figure 3), indicating binding of both ligands to the receptor. Reduction of the STD signals of one ligand upon addition of another suggests that both the ligands bind weakly (K_D µM – mM range, consistent with the measured K_i values[14]) at the same binding site on the receptors.

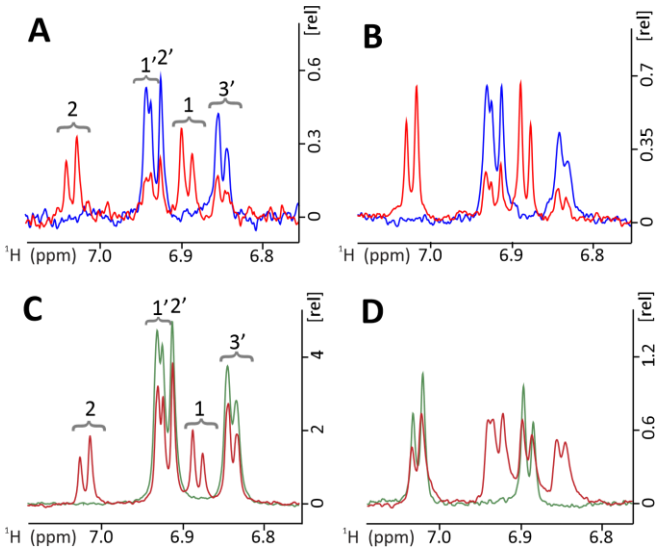

Figure 3. STD competition experiments of epinephrine and norepinephrine with A-61603. (A) STD of 375 µM epinephrine with 2 µM α_{1A}-AR A4 (blue) and upon addition of 375 µM A-61603 (red). (B) STD of 375 µM epinephrine with 10 µM α_{1B}-AR #15 (blue) and upon addition of 375 µM A-61603 (red). (C) STD for 1 mM norepinephrine with 20 µM of α_{1A}-AR A4 (dark green) and upon addition of 500 µM A-61603 (dark-red). (D) STD of 500 µM A-61603 with 10 µM α_{1B}-AR #15 (dark green) and upon addition of 1000 µM norepinephrine (dark-red). All resonances shown here correspond to the phenyl regions of epinephrine, norepinephrine and A-61603 and are labeled according to the structures in Table 1.

Tr-NOESY experiments were then acquired in the presence of two ligands, A-61603 with either epinephrine or norepinephrine and the two receptors (either α_{1A}-AR A4 or α_{1B}-AR #15). In addition to the intraligand NOEs (as shown in Figure 2), several interligand NOE cross-peaks were observed between the resonances of the two ligands when binding to both receptors (Figure 4). The appearance of interligand NOEs between these ligand pairs, which are binding competitively to the receptors, is consistent with an INPHARMA mechanism. It is important, however, to confirm and differentiate such signals from those that may arise from an ILOE mechanism.[18] In ILOE, the two ligands bind simultaneously to neighbouring protein pockets to form a ternary complex, from which the NOEs arise. In the INPHARMA experiment, the ligands bind consecutively to the protein (only binary complexes are formed) and the INPHARMA NOEs originate from a spin-diffusion process via the protons of the protein-binding pocket. Thus, if protein protons are replaced by deuterium, INPHARMA NOEs (and not ILOEs) should be specifically attenuated. To determine the mechanism underlying the interligand NOEs observed in Figure 4, Tr-NOESY build-up experiments were performed on fractionally deuterated receptor under the same experimental conditions. The resulting build-up data and cross-relaxation rates for the intraligand and interligand NOEs were compared against those using the protonated receptor (Figure 5 and Figure S2). Here we expect for INPHARMA that interligand NOEs will be quenched, a consequence to the loss of receptor protons, whereas for ILOE interligand NOEs will be similar in the presence of deuterated receptor. Indeed, for the deuterated receptor interligand NOEs were considerably weaker and thereby built-up more slowly, consistent with INPHARMA. Intraligand NOEs, however, exhibited similar or faster buildup rates, a consequence of fewer pathways for magnetization transfer to the deuterated proteins[26]. To confirm that the NOE cross-peaks form only upon ligand binding to the protein and not from the interaction in solution, NOESY experiments of the ligand pairs, epinephrine/A-61603 and norepinephrine/A-61603, were recorded in the absence of a protein (Figure S3A-B), both the compounds exhibited only positive intraligand NOEs, characteristic of small molecules.

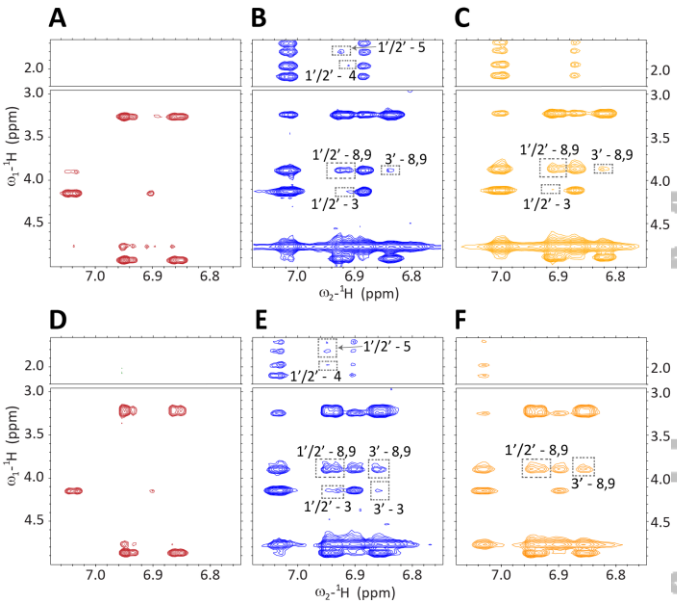

Figure 4. Tr-NOESY experiments of epinephrine and norepinephrine with A-61603. 2D Tr-NOESY spectra of a mixture of 1 mM epinephrine and 0.6 mM A-61603: in the absence of a receptor (A); in the presence of 20 µM α_{1A}-AR A4 (B); and in the presence of 20 µM α_{1B}-AR #15 (C) all recorded with 300 ms mixing time. 2D Tr-NOESY spectra of a mixture of 1 mM norepinephrine and 0.6 mM A-61603: in the absence of a receptor (D); in the presence of 20 µM α_{1A}-AR A4 (E); and in the presence of 20 µM α_{1B}-AR #15 (F); all recorded with 300 ms mixing time. The interligand NOEs (INPHARMA) are highlighted in a dashed line boxes and labeled according to the structures in Table 1, where protons from norepinephrine or epinephrine are denoted by prime symbol (') and protons from A-61603 are not. The colour of the cross peak indicates the phase, positive peaks in dark-red; negative peaks in blue (α_{1A}-AR A4) and in orange (α_{1B}-AR #15).

The occurrence of INPHARMA indicates sequential binding of epinephrine and A-61603 at the same receptor site. This site can either be an orthosteric site i.e. the final binding site for the endogenous agonist[27] or an allosteric site that is topographically distinct from the orthosteric site.[28] Epinephrine/A-61603 Tr-NOESY experiments were repeated in the presence of the high

affinity (prazosin, K_D 8 nM[14]) α_1-AR selective antagonist prazosin, which binds to the orthosteric site.[22d, 29] Upon prazosin addition to α_{1A}-AR A4, all interligand NOEs between epinephrine and A-61603 disappeared, while the intraligand NOEs for these ligands turned positive, representative of unbound ligands, indicating that INPHARMA is occurring at the orthosteric site (Figure S3C). For α_{1B}-AR #15, prazosin addition fully attenuated the interligand NOEs between epinephrine and A-61603, but in contrast to α_{1A}-AR A4, negative intraligand NOEs from both ligands were still observed (Figure S3D). This might indicate non-specific or allosteric binding of the ligands at distinct sites to the orthosteric site. Nonetheless, the absence of interligand NOEs supports that the INPHARMA is resulting from the binding of the two ligands at the orthosteric site on α_{1B}-AR #15.

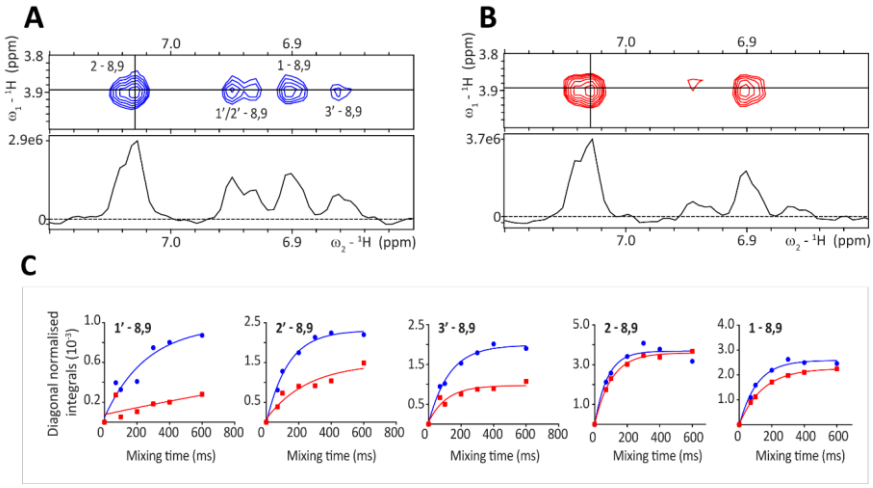

Figure 5. Tr-NOESY experiments with the deuterated receptor. Slices of Tr-NOESY spectra (mixing time 300 ms) for the mixture of 1 mM norepinephrine and 0.6 mM A-61603 in the presence of (A) 20 µM protonated α_{1A}-AR A4 and (B) 20 µM fractionally deuterated α_{1A}-AR A4. (C) Comparison of buildup data of intraligand and interligand NOEs, shown in A and B, of norepinephrine and A-61603 with protonated (in blue) and deuterated (in red) α_{1A}-AR A4 where the decrease in interligand NOEs upon partial deuteration of receptor proves INPHARMA rather than ILOE nature of these interligand NOEs. The first three plots are interligand NOEs between protons of norepinephrine and A-61603, whereas the last two panels are intraligand NOEs for protons of A-61603. All resonances shown here exhibit negative phase and are labeled according to the structures in Table 1.

Determining the binding pose of A-61603 at α_{1A}-AR and α_{1B}-AR. To determine the bound conformations of A-61603 on α_{1A}- and α_{1B}-AR, the INPHARMA data with epinephrine and A-61603 on both α_{1A}-AR A4 and α_{1B}-AR #15 were quantitatively analysed with the SpINPHARMA[30] software. The analyses were performed using the computational models of docked complexes of epinephrine and A-61603 on α_{1A}-AR A4 and α_{1B}-AR #15. Homology models of α_{1A}-AR A4 and α_{1B}-AR #15 were prepared and epinephrine was docked to them (Figure S4A-B) based on the epinephrine bound structure of the β_2-AR[23] and structure-function studies.[22a] Our epinephrine docked models were in good agreement with reported studies where: the *meta*-hydroxyl substituent of the aromatic ring makes hydrogen bonds with $Ser^{5.42x43}$; the *para*-hydroxyl interacts with $Ser^{5.46x461}$; and the protonated amine interacts with $Asp^{3.32x32}$ to both receptors.[22a] The phenyl group contributes significant hydrophobic contacts. The stabilities of the epinephrine docked poses were established by running MD simulations. As indicated by the RMSD plots (Figure S4C) the docked poses of epinephrine were stable on both the α_{1A}-AR A4 and α_{1B}-AR #15 over 500 ns MD simulations.

Initial bound conformations of both enantiomers of A-61603 were created by induced-fit docking into the of α_{1A}-AR A4 and α_{1B}-AR #15 homology models. For each model, 30 poses of each enantiomer were quantitatively scored using SpINPHARMA,[30] which back-calculates the INPHARMA spectra and generates the Pearson correlation coefficient (PCC) values for a pair of ligands based on its agreement with the experimental INPHARMA NOEs. The PCC values of all A-61603 docked poses were calculated against epinephrine docked receptor models (Figure 6A and Figure S5A, S6A and S7A). For both α_{1A}-AR and α_{1B}-AR, the top- and lowest scoring poses of (*R*)- and (*S*)-A-61603 (marked in red in Figure 6A, Figure S5A, 6A and 7A) were subjected to all-atom 100 ns MD simulations to gauge the stability of these receptor-ligand complexes. Ligand RMSD values were analysed and models where the ligand position was stable or stabilising in the course of 100 ns MD simulation were selected for longer 500 ns MD simulations (Figure 6B-C; Figure S5B-C, S6B-C and S7B-C). One hundred frames were sampled from the final 250 ns from each 500 ns simulation. For each receptor subtype, INPHARMA PCC scores were then recalculated between the sampled frames from the A-61603 simulations and the epinephrine simulations, producing a total of 10,000 individual scores for each system. These data, plotted as heat maps, are shown in Figure 6D-J (and Figure S5D-J, S6D-J and S7D-J).

For α_{1A}-AR A4 receptor models, (*R*)-A-61603 conformations, #3, #12 and #25 exhibited overall good PCC values while the low scoring conformation #13 was not stable in the MD simulations. As shown in the Figure S8A, all three poses (#3, #12 and #25) were oriented similarly. Conformation #3 was stable for 500 ns and gave both the highest PCC value (PS_{Max}) of 0.82 (compared to an initial PS_{Max} of 0.72) and the highest median score (PS_{Median}) of 0.43. For (*S*)-A-61603, only conformation #18 exhibited overall good PCC values (Figure S5). The conformation was initially the lowest scoring conformation tested for stability, but during the relaxation phase of MD, the ligand moved to a different position in the receptor (Figure S8B), stabilizing and exhibiting PS_{Max} and PS_{Median} values of 0.58

(compared to an initial PS_{Max} of -0.03) and 0.27 respectively. The five highest scoring snapshots from the simulations of each of the selected conformations i.e. (*R*)-A-61603 #3 and (*S*)-A-61603 #18 are shown in Figure 7B and C respectively with the key interacting residues of the receptor along with the histograms showing the overall distribution of the PCC scores. Based on the overall higher PCC values (PS_{Max} and PS_{Median}) for (*R*)-A-61603 compared to (*S*)-A-61603, the NMR data reflects mostly the binding of the (*R)* enantiomer to α_{1A}-AR. This is consistent with the published work where radioligand binding and functional assays showed that the (*R*) enantiomer of A-61603 is the highly selective enantiomer at WT α_{1A}-AR.[31] Also, the selected conformation #3 of (*R*)-A-61603 on α_{1A}-AR is in a good agreement with the proposed orientation based on STD-NMR build-up studies[14].

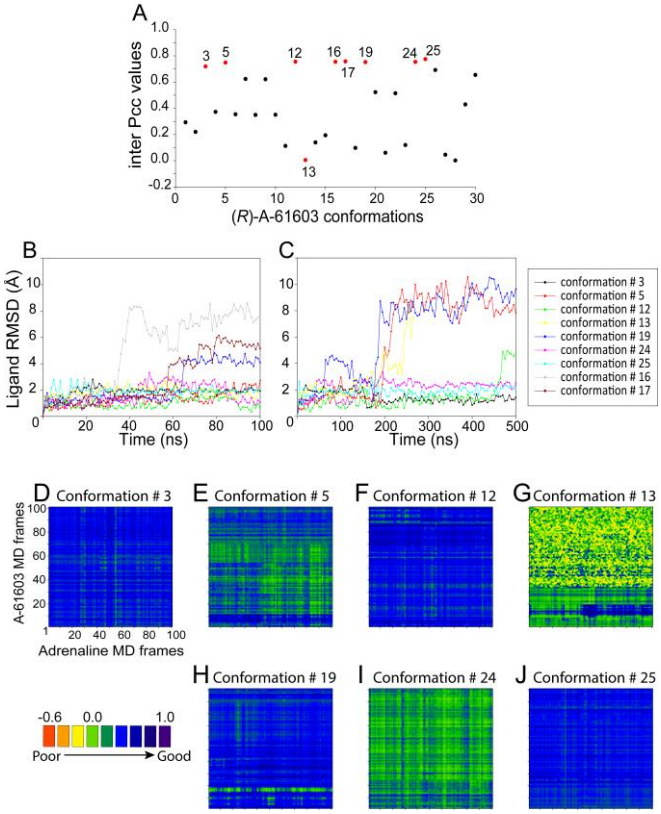

Figure 6. Computational analysis of (*R*)-A-61603 binding to α_{1A}-AR A4. (A) A plot showing INPHARMA PCC (Pearson correlation coefficient) score for each of the 30 (*R*)-A-61603 docked conformations on α_{1A}-AR A4. Selected conformations are marked in red and numbered. (B & C) RMSD plots of the selected (*R*)-A-61603 conformations. (B) RMSD across 100 ns MD simulation. (C) RMSD of the selected stable conformations across 500 ns MD. (D - J) Heat map representing the PCC scores between the extracted MD frames. The values are arranged in temporal order of the epinephrine and A-61603 simulation in the x- and y- dimension, respectively.

A similar analysis was performed for A-61603 binding to the α_{1B}-AR #15 receptor. In this case, (*R*)-A-61603 conformation #23 and (*S*)-A-61603 conformation #17 exhibited the highest PCC values (PS_{Max} of 0.74 (compared to an initial PS_{Max} of 0.67 and 0.69 respectively) for both and PS_{Median} of 0.51 and 0.54 respectively).The lowest scoring conformation of (*R*)-A-61603 was conformation #9 while the lowest scoring pose of (*S*)-A-61603 was conformation #11, both of which were unstable in the simulations (Figure S6 and S7). The top 5 high scoring snapshots of the selected conformations, (*R*)-A-61603 #23 and (*S*)-A-61603 #17, are shown in Figure 7E and F with the key interacting residues of the receptor highlighted. With α_{1B}-AR #15, the PCC values were similar for both top ranked poses for (*R*)- and (*S*)-A-61603, which is consistent with binding studies where each enantiomer exhibited similar affinity at WT α_{1B}-AR.[31]

Effects of mutating residue at position 6.55x55. The proposed conformational poses of A-61603 on α_{1A}-AR A4 and α_{1B}-AR #15 (Figure 7 & Figure S9) suggest that the non-conserved position 6.55x55 (Met292 in α_{1A}-AR and Leu314 in α_{1B}-AR) may play a role in A-61603 sub-type selectivity. Our models suggest that Leu314 in α_{1B}-AR sterically hinders optimal binding of the benzyl group of (*R*)-A-61603, probably explaining the weaker affinity compared to α_{1A}-AR (Figure S10). The hypothesis was tested by shortening the residue at position 6.55x55 in α_{1B}-AR #15 by mutating it to Ala, which resulted in an increased affinity for A-61603, making it similar to α_{1A}-AR A4 as shown in Table 2. As mutating Leu314 to Met in α_{1B}-AR resulted in an increase in the binding affinity of two other α_{1A}-AR selective agonists oxymetazoline and methoxamine,[22b] we investigated the effect of this mutation on the binding of A-61603 to α_{1B}-AR #15, but did not observe any significant increase in the binding affinities for A-61603. We also investigated the effect of mutating Met292 on α_{1A}-AR A4 to Leu, and it resulted in a weaker affinity for A-61603, similar to α_{1B}-AR #15. Effects of these and other mutations on the affinities of A-61603 (as listed in Table 2) supports that the residue at position 6.55x55 plays a role in imparting selectivity to A-61603. Our results suggest, however, that the residue at position 6.55x55 is a major but not the sole contributor of selectivity, as upon mutating Leu314 to Met in α_{1B}-AR did not improve the affinity to the same level as observed for the respective receptor.

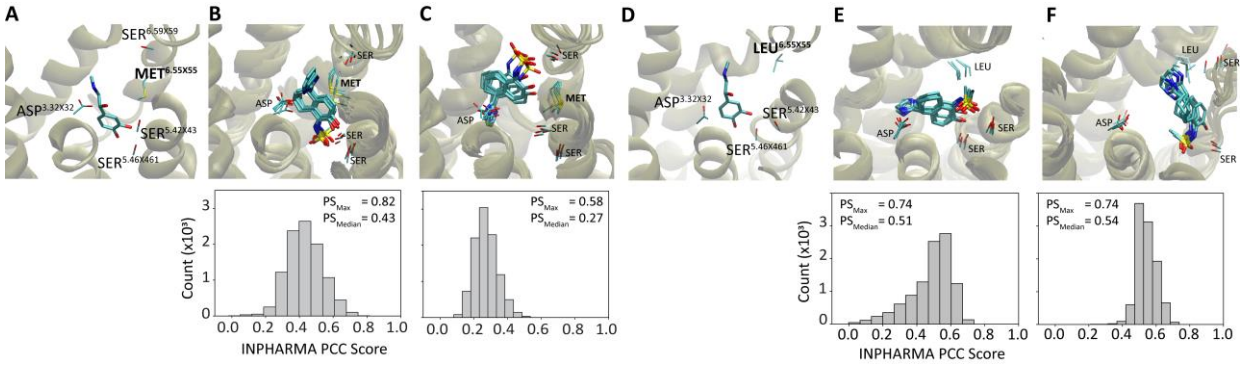

Figure 7. Final predicted conformations of (*R*)- and (*S*)-A-61603 on α_{1A}-AR A4 and α_{1B}-AR #15. Predicted protein-ligand complex structures of the α_{1A}-AR A4 with (A) epinephrine, (B) (*R*)-A-61603 and (C) (*S*)-A-61603. And of the α_{1B}-AR #15 with (D) epinephrine, (E) (*R*)-A-61603 and (F) (*S*)-A-61603. Key protein residues are labelled along with GPCRdb residue numbering in the superscript. Histograms of the INPHARMA PCC scores evaluated for the extracted MD frames are shown for the corresponding (*R*)- and (*S*)-A-61603 conformations, where PS_{Max} is the maximum PCC score and PS_{Median} is the median of the distribution. For all A-61603 poses, the top five high scoring conformations were selected from five equal intervals i.e. from every 50 ns run (out of final 250 ns of 500 ns MD). In other words, from the 100 sampled frames of final 250 ns MD, instead of selecting the five top scoring conformations (which are likely to be clustered together), these 100 frames were sequentially split into five sets of 20 frames. From each set, the highest scoring conformation was selected.

Table 2. Ligand-binding profiles of α_{1A}-AR and α_{1B}-AR mutants.[b]

Receptor mutant	pK_i prazosin	pK_i A-61603
α_{1A}-AR A4	8.0 ± 0.1^{a}	$3.8 \pm 0.1^{a,b,c}$
α_{1A}-AR A4 M292L	7.8 ± 0.1^{b}	$2.6 \pm 0.2^{a,d,e}$
α_{1A}-AR A4 M292A	$7.0 \pm 0.0^{a,b,c,d,e}$	$3.4 \pm 0.2^{d,f,g}$
α_{1B}-AR #15	8.1 ± 0.1^{c}	$2.6 \pm 0.1^{b,f,h}$
α_{1B}-AR #15 L314M	8.0 ± 0.1^{d}	$2.8 \pm 0.1^{c,g,i}$
α_{1B}-AR #15 L314A	7.9 ± 0.1^{e}	$3.5 \pm 0.0^{e,h,i}$

[b] QAPB competition binding (with prazosin/A-61603) against purified α_{1A}-AR and α_{1B}-AR mutants were performed to determine the K_i values as previously described[30] using the receptors solubilized in 0.1% DDM. All binding isotherms were best fit to a single site model. Data represent the mean ± SEM mean from three independent experiments performed in duplicate. The symbols a, b, c, d, e, f, g, h and i indicate statistically different pairs of values in each column based on one-way ANOVA with Tukey multiple comparisons tests.

Discussion

Elucidating the binding modes of ligands to their cognate GPCRs lays the foundation for understanding their biological signaling mechanisms and provides a framework for drug discovery. This study described the application of INPHARMA[19, 32] in determining the bound conformation of an α_{1A}-AR selective agonist, A-61603, at both α_{1A}- and α_{1B}-ARs relative to the predicted bound conformation of an endogenous agonist, epinephrine.[22a, 23] A critical part of our study was to distinguish ILOE from INPHARMA. Typically ILOEs require longer NOE mixing times compared to INPHARMA.[33] But there seems to be no clear consensus as ILOEs have been observed at mixing times ranging from 300-900 ms[18, 34] and INPHARMA NOEs from 70 ms to 600 ms.[20, 32, 35] As the two techniques depend on numerous parameters, we relied upon both competition with a known strong binding ligand[21, 36] and partial deuteration of the receptor.[35b, 35c, 36a] We showed the strong affinity antagonist prazosin competes with both epinephrine and A-61603 in STD-NMR and Tr-NOESY and that fractional deuteration of α_{1A}-AR A4 significantly quenched the interligand NOEs, indicating that the phenomenon we are observing is resulting from INPHARMA, and not ILOE.

Ligand affinities, off-rates and residence times play a pivotal role in observing INPHARMA.[19] INPHARMA NOEs have been mostly observed with ligand pairs with affinities in the µM range and hence, with approximately equal concentrations of two ligands.[32, 36-37] Few studies report optimization of the ligand concentrations according to the relative affinities of the ligands.[20, 38] In a particularly surprising study,[21] INPHARMA NOEs were observed between two ligands with 1000-fold difference in affinities (8.65 µM and 1.60 nM (K_i)) and at equal ligand concentrations. The interligand NOEs with these high affinity binders may be attributed to the high degree of flexibility of the receptor binding pocket leading to increased k_{on} and k_{off} rates.[21] While we were able to observe interligand NOEs with two ligands with 100-fold difference in affinity, it required considerable "tuning" of the experimental and sample conditions; most importantly the ligand and protein concentrations. Ligand concentrations were adjusted according to the relative affinities of the ligands (1000 µM epinephrine and 600 µM A-61603). The INPHARMA experiment was also performed with a mutant of α_{1A}-AR which shows stronger affinities (100-fold) for both epinephrine and A-61603,[14] but for this mutant we could not observe any interligand NOEs. Further optimisation of the experimental conditions may be needed to observe the interligand NOEs with this "high-affinity receptor".

The INPHARMA data is further supported by molecular dynamics simulations and computational analyses to extract energetically reasonable binding poses consistent with the experimental data[21]. Another GPCR study, on GPR40[20] used INPHARMA to determine the relative bound conformations of agonists, without necessarily needing any computational scoring. A reason that could partially account for this success is the use of proton-rich ligands, (~24 protons each ligand) resulting in a substantial number of INPHARMA signals, enough for determining the relative conformations of the ligands. This contrasts with our study where our reference ligand epinephrine has 6 protons and the test ligand A-61603, 16 protons. Our experience with the INPHARMA-SpINPHARMA-MD methodology suggests that it works best with proton rich ligands. We performed similar studies with norepinephrine in place of epinephrine with A-61603. Norepinephrine lacks the methyl group of epinephrine. Although we did observe interligand NOEs between norepinephrine and A-61603, because of the lack of this methyl group we did not obtain sufficient NOEs to definitively select a docked conformation using SpINPHARMA. For better prediction of a bound conformation, a large number of docked complexes should be given as an input in SpINPHARMA. A way to generate such an ensemble of conformations is by performing MD simulations, which, unlike most of the docking algorithms, take into account the flexibility of both the receptor and ligand.[37a] Our studies suggest that the docking poses that scored highly by SpINPHARMA do not necessarily generate poses that are stable in the MD simulations, evident by the high ligand RMSDs in the MD simulations. This instability may be due to the ligand docking being performed on the homology models of the receptors. Cross *et al.*[39] have investigated the effect of input conformation on the accuracy of pose prediction showing

that crystal structures used as an input mostly produced better overall results, when compared to homology models. Since, in our case, there are no crystal structures available for α_{1A}- and α_{1B}-ARs, use of homology models was the best approach. Moreover, the use of all-atom MD simulations and rescoring of the ensembles of scored docked poses enabled us to successfully select the best conformation in agreement with the experimental INPHARMA data, which could be validated by mutagenesis studies. Furthermore, the selected conformations agreed well with the published SAR data.[14]

Conclusion

In conclusion, we have shown that the ligand-based NMR methods are highly useful for the study of weak binding ligands on GPCRs, which are otherwise difficult to study. Providing the sample conditions are optimal and the system requirements are met, the INPHARMA method could prove very useful for the determination of ligand binding poses on GPCRs. These methods can be supported by computational approaches, as done in this work, using SpINPHARMA and MD simulations. Such data would be highly valuable in the absence of direct information about the structure of the receptor, especially for fragment-based drug discovery (FBDD) and the ligand-based drug discovery (LBDD) approaches. Overall, the study shows that the methodology holds great potential in the rational development of subtype-selective drugs in GPCRs.

Experimental Section

General: All samples were prepared as described in Supporting information. The bacterial expression vectors were designed as described elsewhere.[14]

NMR spectroscopy: Unless mentioned otherwise, all NMR samples were prepared containing 20 µM receptor, 1 mM of epinephrine/norepinephrine and/or 600 µM of A-61603 hydrate in 500 µL of phosphate buffer (50 mM Potassium Phosphate, 100 mM NaCl, pH 7.4) containing 0.05% DDM and 10% ^2H_2O in 5-mm NMR tubes. To avoid oxidation, all samples containing epinephrine/norepinephrine were supplemented with 1 mM ascorbic acid. To all samples containing α_{1B}-AR #15, 2 mM CHAPS and 1 mM CHS were added to improve receptor stability over longer time periods.[14]

All spectra were acquired at 25 ºC on a 700 MHz Bruker Avance IIIHD spectrometer equipped with a cryogenically cooled triple resonance probe. 2D Tr-NOESY experiments were acquired using standard pulse sequences with water suppression using excitation sculpting with gradients,[40] 56 scans as 2048 (t2) × 400 (t1) data points at mixing times ranging from 70−800 ms and a relaxation delay of 1.2 s. STD-NMR data were acquired with saturation time of 3 s, using a train of 50 ms Gaussian pulses with a B1 field of 130 Hz, separated by 4 µs delays.[41] The on- and off-resonance frequencies were −1 and 71.4 ppm, respectively. To suppress residual protein and water signals, a spin-lock pulse of 40 ms and excitation sculpting[40] with gradients were employed, respectively. The relaxation delay between transients was set to 3.5 s. A total of 512 transients were averaged over 32,000 data points and a spectral width of 16 ppm. Prior to Fourier transformation, data were multiplied by an exponential function with 2 Hz line-broadening and zero-filled once. Detailed information on the data processing can be found in the Supporting information.

Data were processed and analysed using Bruker Topspin 3.5 or NMRFAM-SPARKY 1.4.[42] The data were apodised with cosine-squared functions in both dimensions and zero-filled to 4096 × 4096 points prior to Fourier transformation. For all 2D Tr-NOESY experiments, data were prepared in the following steps: Based on the two-dimensional (2D) ^{1}H total correlation spectroscopy (TOCSY)[14] and Nuclear Overhauser Effect Spectroscopy (NOESY) spectra[14] all cross and diagonal peaks were assigned and integrated. This measure presented a few difficulties due to peak overlap. Two of these were the 1' and 2' resonances of epinephrine/norepinephrine (numbering shown in Table 1). In the direct dimension, both are overlapping but still distinguishable. Therefore, the volumes were approximated based on the two integration areas (Figure S11). The resonance arising from 1' is a singlet overlapping with a component of the doublet from 2'. Also evident from 1D ^{1}H NMR and Tr-NOESY experiments is the roofing effects between resonances of protons 2' and 3' of epinephrine/norepinephrine, and as a result the outer two transitions have lower intensities than the middle ones, and as calculated for resonance of 3' the downfield peak intensity is 1.25 times the upfield peak. Therefore, the area of the upfield peak of 2' near 6.84 ppm (B) was divided by 1.25, and the obtained value (*x*) was then added to B to obtain the full integral of the resonance of 2'. Accordingly, *x* was subtracted from the integral around 6.86 ppm (A) to obtain the integral of the resonance of 1'. This correction was done for all diagonal intraligand and interligand peaks involving these resonances. In the indirect dimension, both resonances cannot be distinguished. Therefore, the overall integral of both was taken and split relative to the intensity ratios of the corresponding signals on the other side of the diagonal. In this manner we analysed 11, 6 and 5 diagonal peaks of A-61603, epinephrine and norepinephrine respectively; 54, 13 and 8 intraligand NOEs of A-61603, epinephrine and norepinephrine respectively; and 19 interligand NOEs for the epinephrine/A-61603 pair and 14 interligand NOEs for the norepinephrine/A-61603 pair. For the comparison of protonated and deuterated receptor Tr-NOESY data, each cross-peak was normalised by the diagonal peak intensity at 70 ms mixing time in the indirect dimension (F1). All the cross-peaks were then plotted and fitted using Graphpad PRISM 6.01. The initial build-up rates i.e. cross-relaxation rates for all proton pairs (except the ones showing scalar coupling) were then calculated. For α_{1B}-AR #15, differences of the normalized signals between the samples without prazosin and with prazosin were taken into account to remove any signals arising from non-specific binding.

Computational modeling: Homology models of α_{1A}-AR A4 and α_{1B}-AR #15 were built with I-TASSER.[43] The models were processed and refined using the Schrödinger Maestro software suite (version 2018.3) and using the OPLS-2005 force field (FF). The Schrodinger LigPrep was used for geometric optimization of ligands with the OPLS-2005 FF. Ligand ionization states were calculated with Epik.[44] The docked structures were generated using Molsoft ICM-Pro 3.8. and energy minimized using Minimize tool in Maestro version 11.7.012 under OPLS-2005 FF. The System Builder module of the Desmond package[45] was used to embed each receptor model in an explicit water-bilayer-

water environment. The whole system was modelled using the OPLS-2005 FF.

NMR-Computational analysis scheme: The NMR-computational workflow is illustrated in the flow chart shown in Figure 1. Thirty docked conformations of each enantiomer of A-61603 were generated and the PCC scores were calculated using SpINPHARMA[30] for each docked conformation with respect to the docked conformation of epinephrine. A-61603 docked structures exhibiting high PCC values as well as the one with the lowest value, as a control, were selected as starting structures for 100 ns MD simulations. Conformations that were stable or stabilizing during the 100 ns MD were selected for a 500 ns MD simulation. One hundred conformations were sampled from the last 250 ns of the 500 ns MD simulations (i.e. every 2.5 ns). PCC values were calculated between the experimental and back-calculated volumes of the INPHARMA signals for each pair of an epinephrine and A-61603 complex structure resulting in 10,000 values for each conformation. Heatmap plots of the PCC values were produced. The structures exhibiting the highest overall score were selected as the final bound conformations of each ligand. MD trajectories were analysed with VMD[46] and the RMSD plots were generated using the trajectory visualizer tool. Root mean square deviation (RMSD) data and heatmaps were plotted in SigmaPlot 14.0.

More detailed information on computational procedures and PCC scores calculation is included in the Supporting information.

Acknowledgements

We would like to thank Feng-Jie Wu (The University of Melbourne) for assistance with optimizing the expression and purification of receptor samples. We are grateful to Lisa M. Williams and Riley Cridge (The Florey) for assistance with the binding assays. We would also like to thank Prof. Christian Griesinger, Dr. Dirk Bockelmann and Dr. Pablo Trigo Mourino from the Max Planck Institute for Biophysical Chemistry, Göttingen, for kindly providing us the SpINPHARMA software which arose from a collaboration between Max Planck Institute for biophysical chemistry and EMBL (Prof. Teresa Carlomagno). This work was supported by NHMRC project grants 1081801 (D.J.S), 1081844 (P.R.G, D.J.S) and 1141034 (D.J.S, P.R.G). D.J.S. is an NHMRC Boosting Dementia Research Leadership Fellow. T.M.V was supported by a Melbourne International Fee Remission Scholarship (MIFRS) and a Melbourne International Research Scholarship (MIRS).

Keywords: GPCR, INPHARMA, NMR, ILOE, Tr-NOESY

[1] A. J. Venkatakrishnan, X. Deupi, G. Lebon, C. G. Tate, G. F. Schertler, M. M. Babu, *Nature* **2013**, *494*, 185-194.

[2] aR. Santos, O. Ursu, A. Gaulton, A. P. Bento, R. S. Donadi, C. G. Bologa, A. Karlsson, B. Al-Lazikani, A. Hersey, T. I. Oprea, J. P. Overington, *Nat Rev Drug Discov* **2017**, *16*, 19-34; bS. L. Garland, *J Biomol Screen* **2013**, *18*, 947-966.

[3] D. M. Perez, V. A. Doze, *J Recept Signal Transduct Res* **2011**, *31*, 98-110.

[4] aC. R. Chapple, F. Montorsi, T. L. J. Tammela, M. Wirth, E. Koldewijn, E. Fernández Fernández, *European Urology* **2011**, *59*, 342-352; bH. Lepor, L. A. Hill, *Pharmacotherapy: The Journal of Human Pharmacology and Drug Therapy* **2010**, *30*, 1303-1312; cB. G. Katzung, *Basic & clinical pharmacology*, McGraw-Hill Medical, New York, **2012**; dD. J. Buggy, C. K. Power, R. Meeke, S. O'Callaghan, C. Moran, G. T. O'Brien, *British Journal of Anaesthesia* **1998**, *80*, 199-203; eD. A. Johnson, J. G. Hricik, *Pharmacotherapy: The Journal of Human Pharmacology and Drug Therapy* **1993**, *13*, 110S-115S.

[5] aD. M. Perez, M. T. Piascik, N. Malik, R. Gaivin, R. M. Graham, *Molecular Pharmacology* **1994**, *46*, 823-831; bD. M. Perez, M. T. Piascik, R. M. Graham, *Molecular Pharmacology* **1991**, *40*, 876-883; cR. M. Graham, D. M. Perez, J. Hwa, M. T. Piascik, *Circulation Research* **1996**, *78*, 737-749; dD. H. Weinberg, P. Trivedi, C. P. Tan, S. Mitra, A. Perkinsbarrow, D. Borkowski, C. D. Strader, M. Bayne, *Biochemical and Biophysical Research Communications* **1994**, *201*, 1296-1304; eC. Faure, C. Pimoule, G. Vallancien, S. Z. Langer, D. Graham, *Life Sciences* **1994**, *54*, 1595-1605.

[6] aT. Warne, M. J. Serrano-Vega, J. G. Baker, R. Moukhametzianov, P. C. Edwards, R. Henderson, A. G. W. Leslie, C. G. Tate, G. F. X. Schertler, *Nature* **2008**, *454*, 486-491; bS. G. F. Rasmussen, H.-J. Choi, D. M. Rosenbaum, T. S. Kobilka, F. S. Thian, P. C. Edwards, M. Burghammer, V. R. P. Ratnala, R. Sanishvili, R. F. Fischetti, G. F. X. Schertler, W. I. Weis, B. K. Kobilka, *Nature* **2007**, *450*, 383-387.

[7] aO. Cala, F. Guillière, I. Krimm, *Analytical and Bioanalytical Chemistry* **2014**, *406*, 943-956; bM. J. Harner, L. Mueller, K. J. Robbins, M. D. Reily, *Archives of Biochemistry and Biophysics* **2017**, *628*, 132-147; cJ. Qin, O. Vinogradova, A. M. Gronenborn, *Meth. Enzymol.* **2001**, *339*, 377-389; dJ.-P. Renaud, C.-w. Chung, U. H. Danielson, U. Egner, M. Hennig, R. E. Hubbard, H. Nar, *Nature Reviews Drug Discovery* **2016**, *15*, 679-698.

[8] aV. Jayalakshmi, N. R. Krishna, *J. Magn. Reson.* **2002**, *155*, 106-118; bB. Meyer, J. Klein, M. Mayer, R. Meinecke, H. Möller, A. Neffe, O. Schuster, J. Wülfken, Y. Ding, O. Knaie, J. Labbe, M. M. Palcic, O. Hindsgaul, B. Wagner, B. Ernst, (Eds.: A. Hamann, K. Asadullah, A. Schottelius), Springer Berlin Heidelberg, **2004**, pp. 149-167.

[9] aC. Dalvit, P. Pevarello, M. Tatò, M. Veronesi, A. Vulpetti, M. Sundström, *J Biomol NMR* **2000**, *18*, 65-68; bC. Dalvit, G. Fogliatto, A. Stewart, M. Veronesi, B. Stockman, *Journal Of Biomolecular NMR* **2001**, *21*, 349-359.

[10] aG. M. Clore, A. M. Gronenborn, *Journal of Magnetic Resonance (1969)* **1983**, *53*, 423-442; bG. M. Clore, A. M. Gronenborn, *Journal of Magnetic Resonance (1969)* **1982**, *48*, 402-417.

[11] S. Igonet, C. Raingeval, E. Cecon, M. Pučić-Baković, G. Lauc, O. Cala, M. Baranowski, J. Perez, R. Jockers, I. Krimm, A. Jawhari, *Scientific Reports* **2018**, *8*, 8142.

[12] F. M. Assadi-Porter, M. Tonelli, E. Maillet, K. Hallenga, O. Benard, M. Max, J. L. Markley, *Journal of the American Chemical Society* **2008**, *130*, 7212-7213.

[13] B. D. Cox, A. K. Mehta, J. O. DiRaddo, D. C. Liotta, L. J. Wilson, J. P. Snyder, *Biochemical and Biophysical Research Communications* **2015**, *466*, 28-32.

[14] K. J. Yong, M. V. Tasneem, P. J. Shilling, F.-J. Wu, L. M. Williams, M. Deluigi, A. Plückthun, R. A. D. Bathgate, P. R. Gooley, D. J. Scott, *ACS Chem. Biol.* **2018**, *13*, 1090-1102.

[15] D. Brancaccio, D. Diana, S. Di Maro, F. S. Di Leva, S. Tomassi, R. Fattorusso, L. Russo, S. Scala, A. M. Trotta, L. Portella, E. Novellino, L. Marinelli, A. Carotenuto, *Journal of Medicinal Chemistry* **2018**, *61*, 2910-2923.

[16] aP. Balaram, A. A. Bothner-By, E. Breslow, *Journal of the American Chemical Society* **1972**, *94*, 4017-4018; bP. Balaram, A. A. Bothner-By, J. Dadok, *Journal of the American Chemical Society* **1972**, *94*, 4015-4017; cH. N. B. Moseley, E. V. Curto, N. R. Krishna, *Journal of Magnetic Resonance, Series B* **1995**, *108*, 243-261.

[17] J. Plati, N. Tsomaia, A. Piserchio, D. F. Mierke, *Biophys. J.* **2007**, *92*, 535-540.

[18] D. Li, E. F. DeRose, R. E. London, *Journal Of Biomolecular NMR* **1999**, *15*, 71-76.

[19] J. Orts, C. Griesinger, T. Carlomagno, *J Magn Reson* **2009**, *200*, 64-73.

[20] S. Bartoschek, T. Klabunde, E. Defossa, V. Dietrich, S. Stengelin, C. Griesinger, T. Carlomagno, I. Focken, K. U.

Wendt, *Angewandte Chemie International Edition* **2010**, *49*, 1426-1429.
[21] K. Fredriksson, P. Lottmann, S. Hinz, I. Onila, A. Shymanets, C. Harteneck, C. E. Müller, C. Griesinger, T. E. Exner, *Angewandte Chemie International Edition* **2017**, *56*, 5750-5754.
[22] aD. M. Perez, *Biochemical pharmacology* **2007**, *73*, 1051-1062; bJ. Hwa, R. M. Graham, D. M. Perez, *Journal of Biological Chemistry* **1995**, *270*, 23189-23195; cD. J. J. Waugh, M.-M. Zhao, M. J. Zuscik, D. M. Perez, *Journal of Biological Chemistry* **2000**, *275*, 11698-11705; dM. Ahmed, M. Hossain, M. A. Bhuiyan, M. Ishiguro, T. Tanaka, I. Muramatsu, T. Nagatomo, **2008**, *31*, 4.
[23] A. M. Ring, A. Manglik, A. C. Kruse, M. D. Enos, W. I. Weis, K. C. Garcia, B. K. Kobilka, *Nature* **2013**, *502*, 575-579.
[24] S. M. Knepper, S. A. Buckner, M. E. Brune, J. F. DeBernardis, M. D. Meyer, A. A. Hancock, *J. Pharmacol. Exp. Ther.* **1995**, *274*, 97-103.
[25] K. Yong, D. Scott, *Biotechnol Bioeng* **2015**, *112*, 438-446.
[26] R. Pachter, C. H. Arrowsmith, O. Jardetzky, *Journal Of Biomolecular NMR* **1992**, *2*, 183-194.
[27] R. R. Neubig, M. Spedding, T. Kenakin, A. Christopoulos, N. International Union of Pharmacology Committee on Receptor, C. Drug, *Pharmacological Reviews* **2003**, *55*, 597-606.
[28] A. Christopoulos, *Nature Reviews Drug Discovery* **2002**, *1*, 198.
[29] aA. Maïga, M. Dupont, G. Blanchet, E. Marcon, B. Gilquin, D. Servent, N. Gilles, *FEBS Letters* **2014**, *588*, 4613-4619; bM. Ishiguro, Y. Futabayashi, T. Ohnuki, M. Ahmed, I. Muramatsu, T. Nagatomo, *Life Sciences* **2002**, *71*, 2531-2541.
[30] L. Skjærven, L. Codutti, A. Angelini, M. Grimaldi, D. Latek, P. Monecke, M. K. Dreyer, T. Carlomagno, *Journal of the American Chemical Society* **2013**, *135*, 5819-5827.
[31] M. D. Meyer, R. J. Altenbach, A. A. Hancock, S. A. Buckner, S. M. Knepper, J. F. Kerwin, *Journal of Medicinal Chemistry* **1996**, *39*, 4116-4119.
[32] V. M. Sánchez-Pedregal, M. Reese, J. Meiler, M. J. J. Blommers, C. Griesinger, T. Carlomagno, *Angew Chem Int Ed Engl* **2005**, *44*, 4172-4175.
[33] T. Sugiki, K. Furuita, T. Fujiwara, C. Kojima, *Molecules* **2018**, *23*, 148.
[34] aB. Becattini, M. Pellecchia, *Chemistry* **2006**, *12*, 2658-2662; bB. Becattini, C. Culmsee, M. Leone, D. Zhai, X. Zhang, K. J. Crowell, M. F. Rega, S. Landshamer, J. C. Reed, N. Plesnila, M. Pellecchia, *Proc Natl Acad Sci U S A* **2006**, *103*, 12602-12606.
[35] aJ. Orts, S. Bartoschek, C. Griesinger, P. Monecke, T. Carlomagno, *Journal Of Biomolecular NMR* **2012**, *52*, 23-30; bJ. Orts, J. Tuma, M. Reese, S. K. Grimm, P. Monecke, S. Bartoschek, A. Schiffer, K. U. Wendt, C. Griesinger, T. Carlomagno, *Angewandte Chemie International Edition* **2008**, *47*, 7736-7740; cJ. Orts, S. K. Grimm, C. Griesinger, K. U. Wendt, S. Bartoschek, T. Carlomagno, *Chemistry – A European Journal* **2008**, *14*, 7517-7520.
[36] aI. Krimm, *MedChemComm* **2012**, *3*, 605-610; bM. Fruth, A. Plaza, S. Hinsberger, J. H. Sahner, J. Haupenthal, M. Bischoff, R. Jansen, R. Muller, R. W. Hartmann, *ACS Chem Biol* **2014**, *9*, 2656-2663.
[37] aM. Reese, V. M. Sanchez-Pedregal, K. Kubicek, J. Meiler, M. J. Blommers, C. Griesinger, T. Carlomagno, *Angew Chem Int Ed Engl* **2007**, *46*, 1864-1868; bK. Kubicek, S. K. Grimm, J. Orts, F. Sasse, T. Carlomagno, *Angew Chem Int Ed Engl* **2010**, *49*, 4809-4812.
[38] V. M. Sanchez-Pedregal, K. Kubicek, J. Meiler, I. Lyothier, I. Paterson, T. Carlomagno, *Angew Chem Int Ed Engl* **2006**, *45*, 7388-7394.
[39] J. B. Cross, D. C. Thompson, B. K. Rai, J. C. Baber, K. Y. Fan, Y. Hu, C. Humblet, *Journal of Chemical Information and Modeling* **2009**, *49*, 1455-1474.
[40] T. L. Hwang, A. J. Shaka, *Journal of Magnetic Resonance, Series A* **1995**, *112*, 275-279.
[41] M. Mayer, B. Meyer, *Journal of the American Chemical Society* **2001**, *123*, 6108-6117.
[42] W. Lee, M. Tonelli, J. L. Markley, *Bioinformatics* **2014**, *31*, 1325-1327.
[43] Y. Zhang, *BMC Bioinformatics* **2008**, *9*, 40.
[44] J. R. Greenwood, D. Calkins, A. P. Sullivan, J. C. Shelley, *J. Comput. Aided Mol. Des.* **2010**, *24*, 591-604.
[45] K. J. Bowers, D. E. Chow, H. Xu, R. O. Dror, M. P. Eastwood, B. A. Gregersen, J. L. Klepeis, I. Kolossvary, M. A. Moraes, F. D. Sacerdoti, J. K. Salmon, Y. Shan, D. E. Shaw, in *SC '06: Proceedings of the 2006 ACM/IEEE Conference on Supercomputing*, **2006**, pp. 43-43.
[46] W. Humphrey, A. Dalke, K. Schulten, *J Mol Graph* **1996**, *14*, 33-38, 27-28.